

Simulation Model for Low-Speed Bumper-to-Bumper Crashes

2010-01-0051

Published
04/12/2010W. R. Scott, C. Bain, S. J. Manoogian, J. M. Cormier and J. R. Funk
Biodynamic Research Corporation

Copyright © 2010 SAE International

ABSTRACT

The purpose of this study was to develop a numerical analytical model of collinear low-speed bumper-to-bumper crashes and use the model to perform parametric studies of low-speed crashes and to estimate the severity of low-speed crashes that have already occurred. The model treats the car body as a rigid structure and the bumper as a deformable structure attached to the vehicle. The theory used in the model is based on Newton's Laws. The model uses an Impact Force-Deformation (IF-D) function to determine the impact force for a given amount of crush. The IF-D function used in the simulation of a crash that has already occurred can be theoretical or based on the measured force-deflection characteristics of the bumpers of the vehicles that were involved in the actual crash. The restitution of the bumpers is accounted for in a simulated crash through the rebound characteristics of the bumper system in the IF-D function. The output of the model for a numerical simulation is the acceleration vs. time information for each vehicle in the simulated crash. Three low-speed crash tests were performed and the dynamic IF-D curve was measured in each crash. The analytical model was used to simulate the three low-speed crash tests in order to demonstrate the model's ability to describe the vehicle dynamics in a crash that has already occurred. The model is also used to perform parametric studies that show how the structural characteristics of the vehicles' bumpers and the closing speed affect the crash pulse and to demonstrate a technique to estimate the maximum severity of a low-speed crash that has already occurred.

INTRODUCTION

There have been two main approaches to modeling a low-speed collinear crash between two vehicles. The first approach is to treat the vehicles as rigid structures and model the bumpers as spring/dashpot systems and then solve the

governing differential equations with the appropriate initial conditions (1, 3, 4, 7). The solution gives the accelerations of both vehicles during the crash. In order to simulate a specific crash with a spring/dashpot model the appropriate stiffness and damping coefficients must be used. The second approach has been called the Momentum-Energy-Restitution (MER) method. This method is based on rigid body impact mechanics and uses impulse, conservation of momentum, conservation of energy and restitution to determine the ΔV of the vehicles in a low-speed crash (2, 5, 6). In order to estimate the ΔV for a vehicle in a specific crash the MER method requires a value for the coefficient of restitution (ϵ) and an estimate of the energy absorbed by each vehicle during the crash. An analysis of a low-speed crash with the MER method provides a ΔV for the crash but does not provide the acceleration vs. time information for the vehicles during the crash. The peak acceleration in the crash can be estimated by assuming a shape and length for the crash pulse.

Thomson and Romilly (1) treated the vehicle as a rigid mass and the bumper system as a spring/dashpot system in their simulation model. Pendulum-to-car (VW Rabbit) crash tests and static and dynamic compression tests of the VW's piston-type energy absorbers were performed. The simulation model was used to calculate the VWs dynamic response in the pendulum-to-car crash tests. Four different methods were developed to analytically determine the linear coefficients of the spring/dashpot system. The damping and stiffness coefficients that best represented the experimental data were based on an energy analysis of the pendulum-to-car impacts. The calculated accelerations approximated the measured accelerations but did not start at zero because of the constant coefficient for the dashpot.

Bailey et al. (2) performed a series of car-to-car crash tests with vehicles whose bumpers had piston-type energy absorbers. The MER method was used to calculate the ΔV of

the vehicles in the crash tests. In the ΔV calculations ϵ was based on previously performed barrier impacts with the same vehicles and the energy absorbed by each vehicle was estimated from the amount of compression of the piston-type energy absorber in the actual crash test. The ΔV s calculated with the MER method were very close to the ΔV s measured in the crash tests.

Ojalvo and Cohen (3) reviewed vehicle-to-vehicle crash test data of Ford Escorts that had bumpers with piston-type energy absorbers and concluded that a linear spring/dashpot model could be used to represent the dynamic response of these vehicles in low-speed crashes. In their model the vehicles were rigid masses and the bumpers were linear spring/dashpot systems. The simulation model was used to produce closed form solutions of the vehicle accelerations in the vehicle-to-vehicle crash tests. The spring and viscous damping coefficients used in simulations were based on the crash test data. The calculated accelerations matched the measured accelerations very well except at the start of the crash where the calculated accelerations were non-zero because of the constant coefficient for the dashpot. A follow-up study by Ojalvo et al.(4) used this simulation model to simulate low-speed crash tests between cars with bumpers that had foam-type and honeycomb-type energy absorbers as well as the piston-type energy absorbers.

Cipriani et al. (5) used a modified MER method to calculate an upper limit to the ΔV experienced by a vehicle in a low-speed crash. A series of 30 low-speed collinear crash tests were performed with vehicles that had bumpers with foam-type and piston-type energy absorbers. Functions of restitution (ϵ) vs. closing speed were developed for the different bumper configurations based on their crash test data and previously published data. The modified MER method was used to estimate the ΔV s of the vehicles in the crash tests. The estimation of a crash test ΔV was made by obtaining ϵ from the appropriate restitution function and the energy absorbed by each vehicle was calculated using bumper stiffness coefficients (A and B coefficients obtained from published data) and a conservative estimate of the crush on the crash test vehicle. The calculated ΔV s were generally greater than the ΔV s measured in the crash tests (probably because of an overestimate of absorbed energy). This modified MER method provides a technique to estimate the upper limit of the ΔV in a low-speed crash.

Happer et al. (6) developed a technique for quantifying the severity of low-speed impacts involving little or no vehicular damage using the MER method. Sixty-nine barrier tests and vehicle-to-vehicle tests were performed in order to develop and evaluate the technique. The technique to calculate a ΔV for a vehicle in a low-speed vehicle-to-vehicle crash involved nine steps. In the ΔV calculation the appropriate restitution function from Cipriani et al. (5) was used to obtain the value of ϵ and the energy absorbed by each vehicle was determined

by relating the crash test vehicle damage to the damage that same model experienced in the barrier tests. The technique presented in this study provides a good method of estimating the crash severity (ΔV) of vehicles in low-speed collisions.

Brach (7) developed a nonlinear spring/dashpot model of low-speed vehicle-to-vehicle crashes. The nonlinear spring and dashpot each had a coefficient and an exponent in the governing equations. During the development of the model, the author determined that the damping during the restitution (rebound) phase of an impact was greater than the damping during the initial compression phase; therefore the damping coefficient was greater during the restitution phase than the compression phase of a simulated impact. The damping force was also proportional to the product of the relative velocity and the relative displacement of the dashpot so that the damping force did not rise instantaneously once the vehicles made contact. This nonlinear spring/dashpot model was used to simulate published crash test data and the coefficients and exponents were selected so that the calculated accelerations matched the measured accelerations throughout the crash pulse of the simulated crash. In the simulations the accelerations were zero at the time of initial contact because the damping force was proportional to the displacement of the dashpot.

The objective of the research described in this paper was to develop a numerical low-speed impact model that could simulate low-speed collinear vehicle-to-vehicle impacts where the impact force could be directly related to the physical properties of the bumpers that were involved in the crash. This approach allows the crash severity of a low-speed crash involving specific vehicles to be estimated and allows a parametric analysis of the crash to determine how different variables affect the crash pulse. This approach also takes into account the considerable variability of the force-deformation characteristics of the bumper systems that are on present day vehicles.

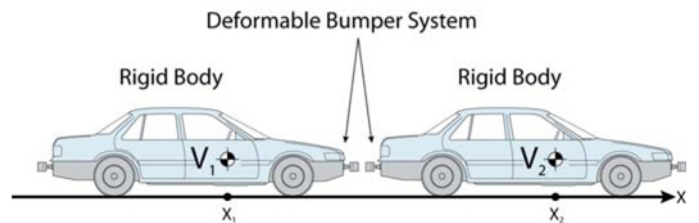


Figure 1. A schematic of the physical system that the model represents.

METHODS

ANALYTICAL MODEL

The model presented is intended to simulate a collinear impact between two vehicles, Vehicle 1 (bullet vehicle) and

Vehicle 2 (target vehicle), with masses M_1 and M_2 . As shown in Fig. 1, the model assumes that the vehicle bodies are rigid structures and the only part of the vehicles that deform are the bumper systems. The numerical simulation satisfies Newton's Second Law at discrete time positions j ,

$$F_j = M_i A_{i,j} = M_i (V_{i,j} - V_{i,j-1}) / \Delta t \quad (i=1,2) \quad (1)$$

where F_j is the impact force, $A_{i,j}$ is the vehicle acceleration, $V_{i,j}$ is the vehicle's velocity, Δt is the numerical time step and the i subscript denotes the vehicle number and the j subscript denotes the discrete time position. The time t is defined as $t = (j-1)\Delta t$ and the crash starts at $t = 0$.

The simulation starts with the vehicles in contact at $t = 0$ and then marches forward in time with time step Δt . The variables calculated at each discrete time position are the location of each vehicle's center of mass ($X_{i,j}$) and each vehicle's velocity ($V_{i,j}$). The impact forces ($F_{i,j}$) and the resulting accelerations ($A_{i,j}$) act on each vehicle during the Δt period between each discrete time position. The structural characteristics of both vehicles' bumpers are combined and input as a system Impact Force-Deformation (IF-D) function where Deformation is the sum of the deformation of the two bumpers. The Impact Force-Deformation function can be a theoretical curve or based on measured force-deflection data for specific bumpers. The output of the simulation is the acceleration versus time information for each vehicle. The algorithm presented here was programmed in MATLAB 7.0 (The MathWorks, Inc).

The numerical simulation starts at $t=0$ ($j=1$) with the vehicles in contact and the initial conditions required are vehicle speeds ($V_{1,1}, V_{2,1}$), and the center of mass positions ($X_{1,1}, X_{2,1}$) along the line the vehicles are traveling. Since the vehicles are in contact but not deformed at time $t = 0$ the undeformed distance (UD) between the two centers of mass is

$$UD = X_{2,1} - X_{1,1} \quad (2)$$

At the first time position $A_{1,1} = A_{2,1} = 0$, and the vehicles move forward through the first time step at their initial velocities and the velocities at the second time position ($j=2$) are the same as the initial conditions, $V_{1,1} = V_{1,2}$ and $V_{2,1} = V_{2,2}$. At the second time position the vehicles' center of mass positions are

$$X_{i,2} = X_{i,1} + V_{i,1} \Delta t \quad (i=1,2) \quad (3)$$

This movement of the center of mass of each vehicle creates an overlap of the vehicles, and the deformation (D_j) at the second and following time positions ($j \geq 2$) is

$$D_j = UD - (X_{2,j} - X_{1,j}) \quad (4)$$

The impact force $F_{i,j}$ that acts on each vehicle during the j^{th} time step ($j \geq 2$) is based on the input IF-D function and Newton's Third Law,

$$-F_{1,j} = F_{2,j} = \text{Function}(D_j) \quad (5)$$

The force $F_{i,j}$ ($i=1,2$) acts on the vehicles during the j^{th} time step where $j \geq 2$. Newton's Second Law is used to calculate the acceleration of each vehicle during the j^{th} time step,

$$A_{i,j} = F_{i,j} / M_i \quad (i=1,2) \quad (6)$$

The impact forces accelerate the vehicles over the j^{th} time step. The time position is incremented, $j = j+1$, and the velocities at the new time position j are calculated,

$$V_{i,j} = V_{i,j-1} + A_{i,j-1} \Delta t \quad (i=1,2) \quad (7)$$

The algorithm then checks to see if the vehicles have reached a common velocity. If the vehicles have reached a common velocity Function (D_j) is changed to represent the rebound phase of the input IF-D function (see Appendix A). The simulation then calculates the vehicle center of mass positions at the new time position,

$$X_{i,j} = X_{i,j-1} + V_{i,j-1} \Delta t + \frac{1}{2} A_{i,j-1} \Delta t^2 \quad (i=1,2) \quad (8)$$

The simulation then recalculates the variables in Eq. 4,5,6,7,Eq. 8 and continues to move forward in time until $F_{i,j}$ ($i=1,2$) in Eq. 5 reaches zero and the crash is over.

The restitution of the crushed structures in a low-speed crash is usually accounted for by assigning a coefficient of restitution (ε) to the crash which is defined as the ratio of the separation velocity to the closing velocity,

$$\varepsilon = (V_1^* - V_2^*) / (V_1 - V_2) \quad (9)$$

where V_1 and V_2 are the pre-crash velocities and V_1^* and V_2^* are the post-crash velocities of the vehicles. The standard method of estimating ϵ for a low-speed crash is to perform a low-speed crash test and calculate ϵ using Eq. 9. Our model accounts for restitution through the Impact Force - Deformation function. This approach is based on the energy definition of ϵ ,

$$\epsilon^2 = E_{afc}^* / E_{afc} \quad (10)$$

where E_{afc} is the energy in the two vehicle system available for crush prior to the crash and E_{afc}^* is the energy available after the crash (8). The theoretical basis for this approach is given in Appendix A.

The accuracy of this numerical analytical model is a function of the magnitude of the time step Δt . A suitable Δt was chosen by using the model to calculate the crash pulse for a purely elastic crash. For this simulation $V_1=10$ ft/sec and $V_2=0$, $M_1 = M_2 = 3500$ lb/g where g is the acceleration due to gravity ($g = 32.2$ ft/sec²). The IF-D function used in this simulation is based on the measured force-deformation curve of the front bumper of a 2007 Ford Edge that is shown in Fig. B3. A description of the Ford Edge's front bumper and the measurement of its force-deformation characteristics are given in Appendix B. For simplicity the force-deflection curve of this bumper is taken to be a straight line that has a slope of 48,000 lbs/ft of deformation. This linear force-deflection curve is shown in Fig. B3 as a dashed line.

Both bumpers in this simulation are taken to have the same structural characteristics. If two bumpers are aligned in series with each other and both have linear force deflection characteristics defined by a slope (S_1 and S_2), then the force-deflection curve of the system has a slope that is defined by,

$$S_{system} = 1 / (1/S_1 + 1/S_2) \quad (11)$$

Therefore, the system IF-D function for this simulation is a straight line with a slope of 24,000 lbs/ft. This curve is shown in Fig. B3 as a solid straight line.

The crash that was simulated in order to evaluate the magnitude of the time step was taken to be completely elastic. Since the vehicle masses are equal the correct post-crash velocities are $V_1^*=0$ and $V_2^*=10$ ft/sec for this elastic impact. Table 1 shows the pulse durations and the post-crash velocities for a range of Δt s used in this numerical simulation. The magnitude of the time step had little effect on the calculated duration of the crash but it did influence the calculated post-crash velocities. A $\Delta t = 0.00001$ sec provided calculated post-crash velocities with only 0.01% error and

reasonable computing time, therefore this time step was used in the simulations discussed in this study.

TABLE 1. Calculated pulse duration and post-crash velocities for Δt s of different magnitude.

Δt (sec)	Pulse Duration (sec)	V_1^* (ft/sec)	V_2^* (ft/sec)	% Error in V_1^*
0.001000	0.1500	-0.082	10.082	0.82%
0.000500	0.1495	-0.041	10.041	0.41%
0.000100	0.1495	-0.008	10.008	0.08%
0.000050	0.1495	-0.004	10.004	0.04%
0.000010	0.1495	-0.001	10.001	0.01%
0.000005	0.1495	-0.000	10.000	0.00%

LOW-SPEED BUMPER-TO-BUMPER CRASH TESTS

The numerical model does not have to be validated in the sense that it is based on Newton's Second and Third Laws but the model's ability to recreate a crash that has already occurred needs to be demonstrated. The simulation model is used to simulate the dynamics of the target and bullet vehicle in three low-speed bumper-to-bumper crashes. The IF-D function used in the simulations is similar to the IF-D curve measured during the crash. A description of each bumper used in the crash tests is given in Appendix B along with the quasi-static force-deformation characteristics for that bumper.

The low-speed crash tests were performed with two vehicles that had been modified for low-speed bumper-to-bumper impacts. A schematic of the test setup is shown in Fig. 2. Vehicle 1 (bullet vehicle) is a 2003 Ford Explorer that had a test weight of 4246 lbs. The Explorer had a steel plate rigidly attached to the frame at the front and a 2007 Ford Edge front bumper was mounted onto this steel plate. Vehicle 2 (target vehicle) was a buck made from a pickup frame that had a test weight of 3382 lbs. A significant part of the mass of Vehicle 2 came from weights rigidly attached to the pickup frame. Vehicle 2 had a steel plate rigidly attached to the rear of the frame and six load cells (Model 1210AO, 10 klbs, Interface, Inc.) were attached to this plate and a second steel plate was attached to the other end of the load cells. The rear bumper of a 2007 Kia Sportage was mounted onto the rearmost steel plate at a vertical position that provided full engagement with the front bumper on Vehicle 1. A description of the rear bumper of the 2007 Kia Sportage is given in Appendix B. A

Table 2. The pre-impact velocities, the post-impact velocities, the ΔV s experienced by each vehicle in the crash tests and the coefficient of restitution calculated using the velocity and energy definition for ϵ in each of the crash tests.

Test No.	V_1 (ft/sec)	V_2 (ft/sec)	V_1^* (ft/sec)	V_2^* (ft/sec)	ΔV_1 (ft/sec)	ΔV_2 (ft/sec)	$\epsilon_{\text{velocity}}$	ϵ_{energy}
1	2.9	0	0.9	2.7	-2.0	2.7	0.62	0.68
2	4.3	0	1.4	3.8	-2.9	3.8	0.56	0.62
3	5.9	0	2.0	5.0	-3.9	5.0	0.51	0.53

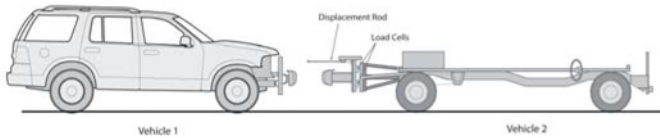


Figure 2. A schematic of the test set up for the low-speed bumper-to-bumper crash tests.

displacement rod extended from the rear plate on Vehicle 2. A string pot (Model PT101, 10 inch, Celesco, Inc.) was mounted on the steel plate and the string was attached to the end of the rod. Just before the vehicles' bumpers made contact the displacement rod contacted the steel plate on the front of Vehicle 1 and the rod was compressed. The string pot measured the distance the displacement rod was compressed. Both vehicles had accelerometers (Model 7596-10/30, Endevco Corporation) mounted on the frames to measure the accelerations in the three vehicle axis. The impact speed of the bullet vehicle (Vehicle 1) was measured with an infra-red sensor (model SM312LVMHS, Banner, Inc.) and retro-reflective tape (Banner, Inc.) and also with high-speed digital video recordings (1000 frames/sec). The data was sampled at 5000 HZ (16-channel TDAS-PRO, DTS, Inc.).

Three low-speed tests were performed. The impact speed of Vehicle 1 (bullet) was 2.9, 4.3 and 5.9 ft/sec. Vehicle 1 achieved its velocity by rolling down a ramp with its engine off. Vehicle 2 was stationary pre-impact for all tests and its wheels were free to roll. The data measured in each test were the impact speed of Vehicle 1, the vehicle accelerations, the impact force (sum of the six load cells), and the distance between the steel plates on Vehicle 1 and 2. The acceleration data were filtered (SAE J211/1, CFC 60). The impact bars on the bumpers were measured after each test with a measuring arm (Model C0605, FARO, Inc), but there was no permanent damage to the impact bars and they were not replaced. The only damage was to the plastic honeycomb energy absorber on the Edge bumper and this was replaced after each test. The foam structure on the top of the Sportage's impact bar was not damaged in any of the crash tests and was not replaced. The vehicle velocities were calculated using the initial speeds and integrating the measured accelerometer data over time. [Table 2](#) is an overview of the velocity measurements made in the three crash tests and the coefficient of restitution calculated using the velocity definition (Eq. 9) and using the energy definition (Eq. 10) with the measured IF-D curves that are shown in [Fig. 3](#). The coefficients of restitution calculated

with the energy definition were slightly higher than the coefficients of restitution calculated with the velocity definition.

<table 2 here>

[Figure 3](#) shows the dynamic IF-D curves created from the measured load cell and displacement rod data for each of the tests. The deformation data is the sum of the deformation of the bumper on the target vehicle and the deformation of the bumper on the bullet vehicle. The slopes of the three curves during the compression phase are very similar. In Tests 1 and 2 the impact force reached a peak and the deformation began to decrease after the peak force was reached. In Test 3 the force remained constant at approximately 9000 lbs then decreased and increased again before the deformation began to decrease. During the rebound phase there was less energy recovered as a percentage of the maximum crush energy as the impact speed increased. This is reflected in the decreasing value of ϵ calculated with the energy definition of ϵ shown in [Table 2](#). The maximum deformation occurred as the impact force was decreasing in the IF-D curves for all these tests.

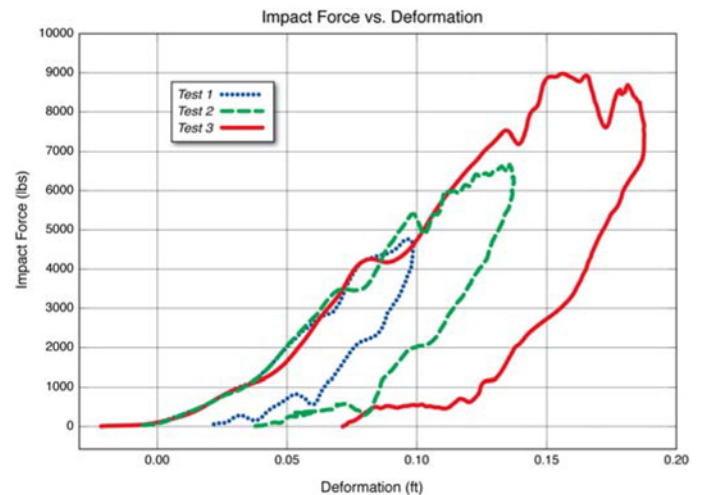


Figure 3. The Impact Force vs. Deformation (IF-D) curves made from the measured load cell data and displacement rod data for Crash Tests 1, 2 and 3.

[Figure 4](#) shows the measured accelerations for the target and bullet vehicles along with the accelerations for each vehicle calculated with the load cell measurements, the vehicle masses and Newton's Second Law. The acceleration data for

the buck (target vehicle) had lower amplitude vibrations than the acceleration data for the Ford Explorer (bullet vehicle). The magnitude of the accelerations calculated with the force data is lower than the magnitude of the accelerations measured on the target and the bullet vehicle over most of the crash pulse. From an experimental standpoint these differences are acceptable; however these differences will have an affect in the simulation calculations when the IF-D curves in Fig. 3 are input into the simulation model because one of the requirements of the simulation model is that at maximum crush the target and bullet vehicles be at a common velocity. When the IF-D curves in Fig. 3 and the appropriate pre-impact speeds and vehicle masses are input into the simulation model the vehicles do not reach a common velocity at maximum crush and the simulation cannot be completed. In order to calculate the crash test acceleration profiles with the simulation model the measured IF-D curves shown in Fig. 3 had to be modified. The modification was to multiply the impact force by a constant so that at maximum crush the bullet and target vehicles reached a common velocity. The modifying constant was found by performing an iteration procedure during the compression phase of the crash in the simulation. The modifying constants for Crash Tests 1, 2 and 3 were 1.14, 1.18 and 1.16 respectively. Figure 5 shows the measured IF-D curves (same as in Fig. 3) and the modified curves that were used in the simulations. This modification is probably needed because of the assumption that both vehicles are rigid masses and response time differences between the load cells and accelerometers.

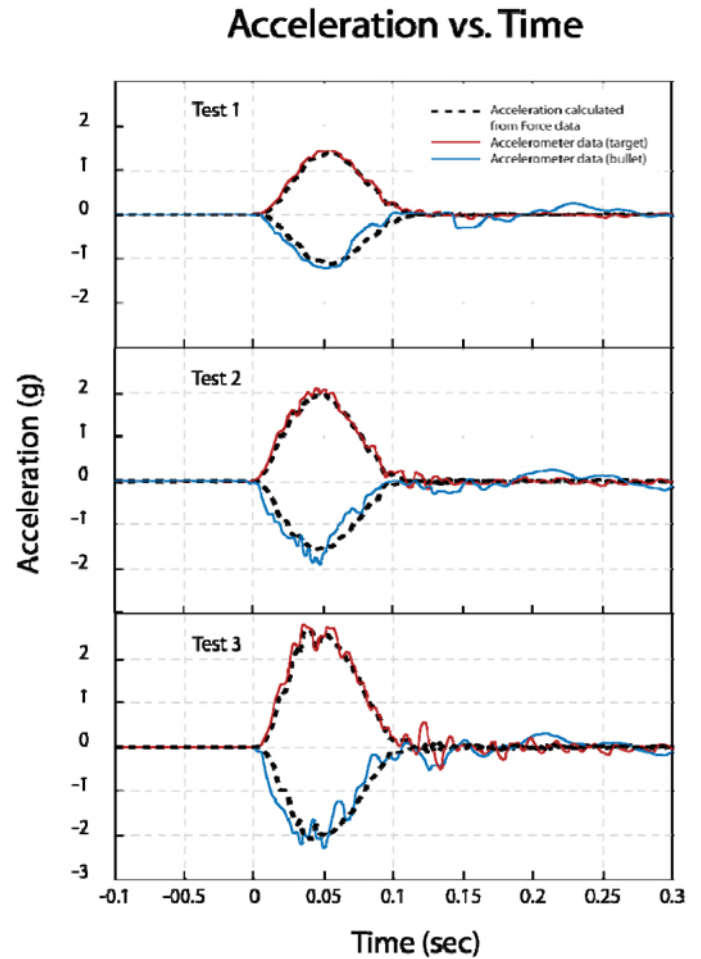


Figure 4. The Acceleration vs. Time data measured in the target and bullet vehicle in the three crash tests. The dashed lines are the accelerations calculated from the load cell data and the solid lines are the accelerations measured by the accelerometers in each vehicle. The accelerations for the target vehicle are positive and accelerations for the bullet vehicle are negative

Impact Force Deformation Curves

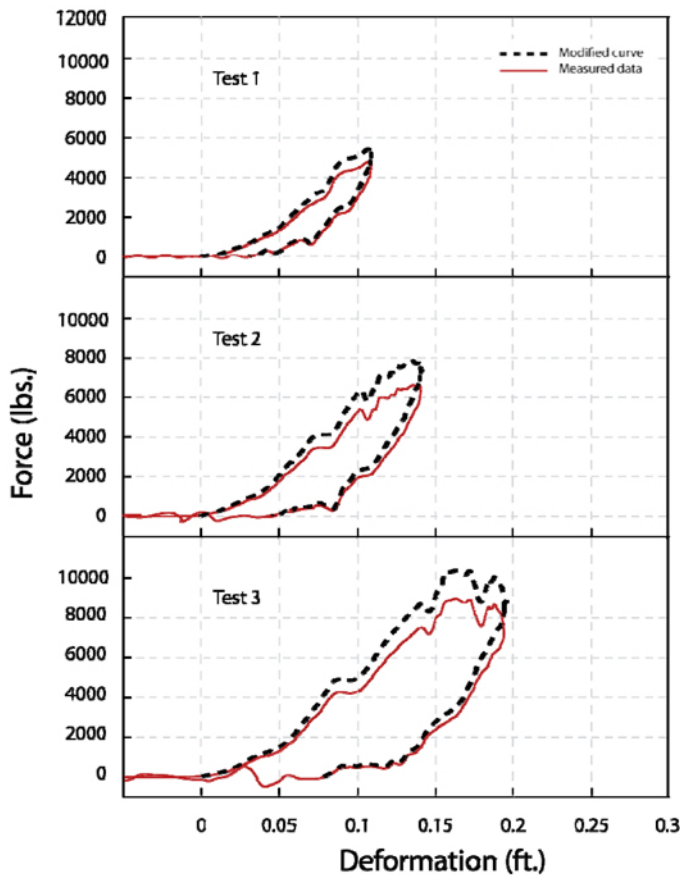


Figure 5. The measured IF-D curves are shown as solid lines and the modified IF-D curves used in the simulations are shown as dashed lines.

RESULTS

SIMULATION OF CRASH TESTS

Figure 6 shows the measured accelerations and the accelerations calculated with the simulation model for the three crash tests. The calculated accelerations match the measured accelerations very well. Also the calculated duration of the crash is approximately equal to the measured duration. Figure 7 shows the velocities calculated with the simulation model for the three crash tests. The crash velocities were obtained by using the pre-impact speeds and integrating the accelerations, either measured or calculated, over time. The calculated velocities match the measured velocities very well. The calculated ΔV s at 120 ms for the target vehicle were essentially the same as the measured ΔV s. The calculated ΔV s at 120 ms for the bullet vehicle were 4 to 6% greater than the measured ΔV s but this difference appeared to be due to the amplitude of the vibrations in the bullet vehicle acceleration data. The good comparisons between the measured and calculated accelerations indicate

that when the appropriate IF-D function is input into the analytical model the model can accurately simulate the dynamics of the bullet and target vehicle.

PARAMETRIC STUDIES

The first parametric study performed with the analytical model varied the restitution in a two vehicle crash while keeping all of the other variables constant. The initial conditions were $V_1=10$ ft/sec and $V_2=0$ ft/sec and the vehicle masses, M_1 and M_2 , were both 3500 lb/g. The simulations were performed using the linear force-deformation curve in Fig. B3 (slope= 48,000 lb/ft) to represent the bumper characteristics of both vehicles during the crushing phase of the crash. Therefore the compression phase of the system IF-D function was linear and had a slope of 24,000 lb/ft. The rebound phase of the IF-D function was also linear and the slope was varied to reflect values of ϵ that ranged from 0.0 to 1.0 (see Appendix A). The rebound IF-D functions used are shown in Fig. 8. Based on Eq. 10 other shapes for the rebound functions could have been chosen, but for simplicity the rebound IF-D functions in this parametric study and the following parametric studies have been represented as straight lines.

The calculated acceleration vs. time curves for the target vehicle, Vehicle 2, are shown in Fig. 9. The effect of increasing restitution is to extend the pulse duration. The duration of the crash doubles from 0.0748 secs in the inelastic crash ($\epsilon=0$) to 0.1495 secs in the elastic crash ($\epsilon=1.0$). The crash pulses in Fig. 9 also show that up until the common velocity of 5 ft/sec is reached at 0.0748 secs the crash pulses are the same, a result of the similar IF-D function used up to that point in the simulation. Once the common velocity is reached the bumpers with the greater restitution continue to apply impact forces, and the crash pulse continues.

The second parametric study looked at the effect of bumper stiffness on the crash pulse. This parametric study was performed with the initial conditions $V_1=10$ ft/sec and $V_2 = 0$ ft/sec, and $M_1= M_2 = 3500$ lb/g. The phases of the system IF-D functions were represented as straight lines with slopes that ranged from 12,000 to 72,000 lb/ft of deformation. The rebound phases of the system IF-D function for each simulation were taken to be straight lines with a slope that resulted in $\epsilon = 0.4$. With ϵ defined, the post-crash velocities and the vehicle ΔV s were the same for each simulation in this parametric study ($V_1^*= 3$ ft/sec, $V_2^*= 7$ ft/sec, $\Delta V_1= -7.0$ ft/sec, $\Delta V_2 = 7$ ft/sec). Figure 10 shows how changing the bumper stiffness affected the calculated crash pulses. This parametric study indicates that while the ΔV s were the same in each simulated crash, the magnitude of the accelerations were dependent on the bumper stiffness. Increasing the stiffness shortens the duration of the crash and increases the peak acceleration. Decreasing the stiffness increases the

duration of the crash pulse and decreases the peak acceleration.

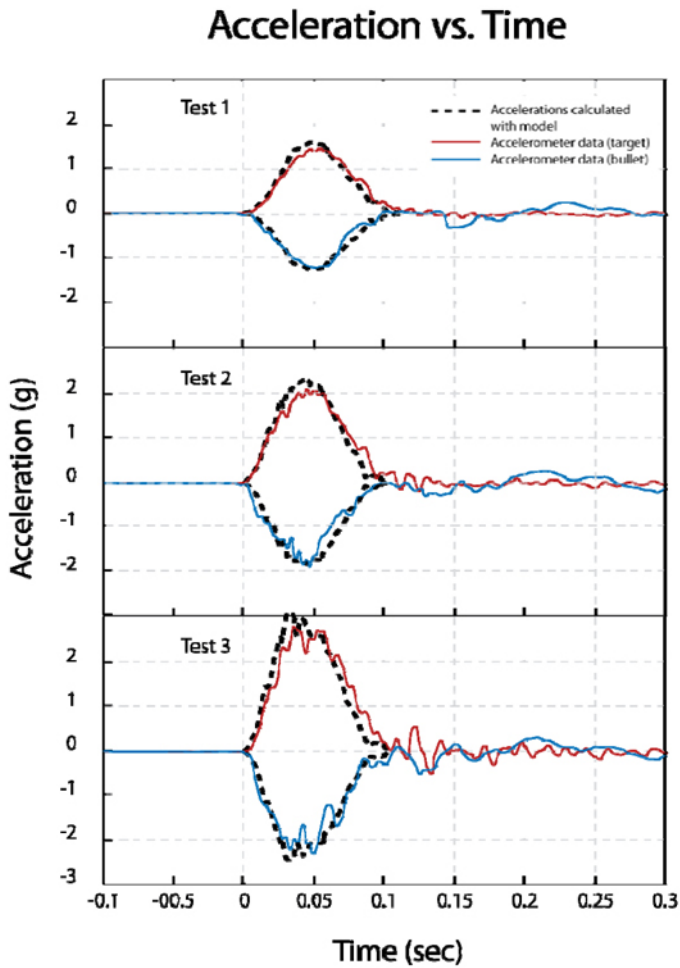


Figure 6. The Acceleration vs. Time curves for the three crash tests. The measured accelerations are solid lines and the accelerations calculated with the simulation model are dashed lines. The accelerations for the bullet vehicle (Vehicle 1) are negative during the crash and the accelerations for the target vehicle (Vehicle 2) are positive.

Velocity vs. Time

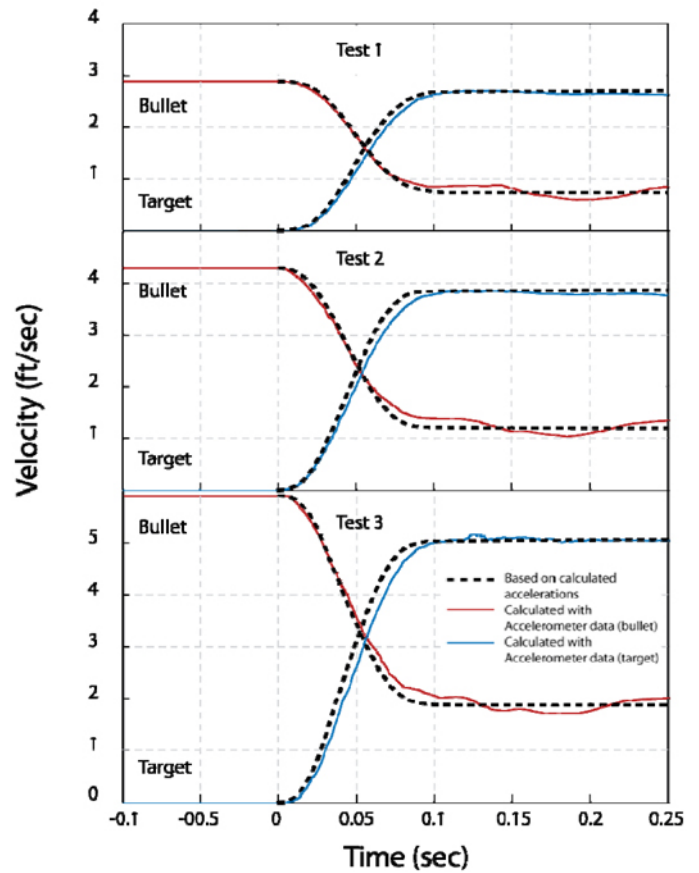


Figure 7. The Velocity vs. Time curves for the three crash tests. The velocities based on the measured accelerations are shown as solid lines and the velocities calculated with the simulation model are shown as dashed lines.

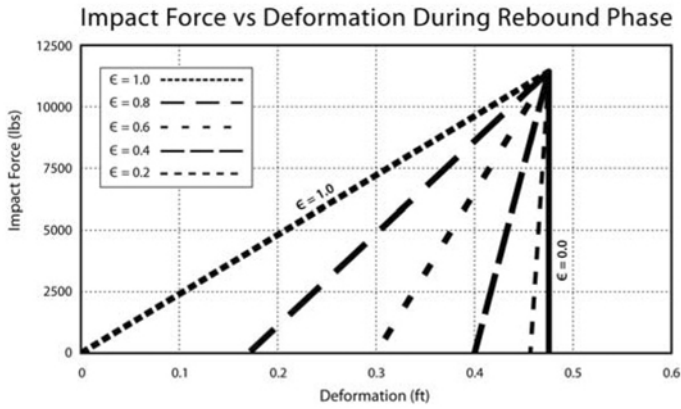


Figure 8. The rebound IF-D functions used in the parametric study where ϵ was varied. In these rebound curves the deformation curve starts at maximum crush (0.47 ft) and then moves to the left as the bumper structures rebound.

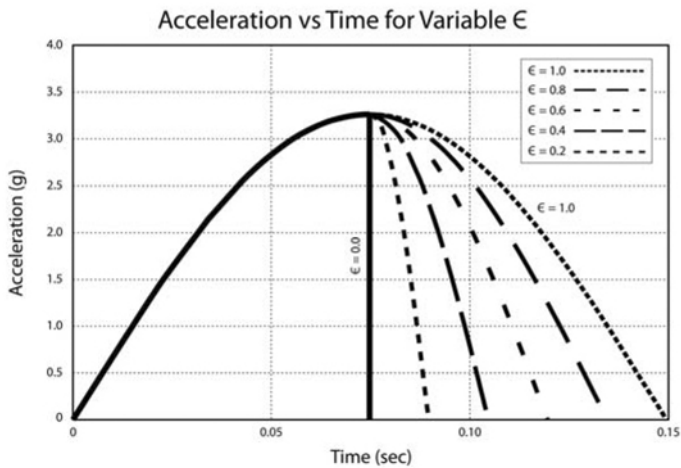


Figure 9. The calculated Acceleration vs. Time curves for the target vehicle in crashes with different ϵ .

The third parametric study varied the closing speed and kept the other parameters the same. Both vehicles had the same mass ($M_1=M_2=3500\text{lb/g}$) in this parametric study. The compression phase of the IF-D function was a straight line with a slope of 24,000 lb/ft and the rebound phase was a straight line that represented an ϵ of 0.4 (see Fig. 8). The calculated crash pulses are shown in Fig.11. For a given stiffness and the same relative amount of restitution the duration of the pulse was the same for the different closing speeds. Increasing the closing speed increased the magnitude of the accelerations produced in the crash, but it did not change the duration of the pulse.

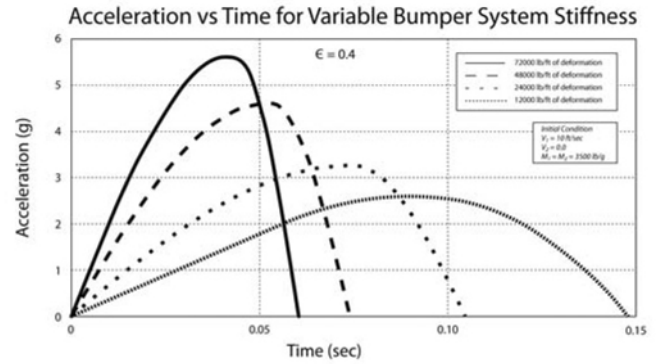


Figure 10. The calculated Acceleration vs. Time curves for the target vehicle in crashes with different bumper stiffness.

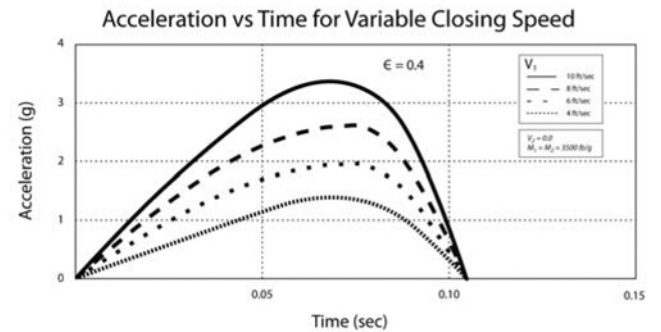


Figure 11. The calculated Acceleration vs. Time curves for the target vehicle for different closing speeds.

TECHNIQUE TO ESTIMATE PEAK ACCELERATION

One of the applications of this numerical analytical model is to estimate the peak acceleration experienced by a vehicle in a low-speed bumper-to-bumper crash where there is little or no damage to the bumpers involved in the crash. There are two steps in this analysis. The first step is to measure the force-deflection characteristics of the bumper systems involved in the crash. Both bumper systems should be compressed until there is a structural failure of a component of the bumper system, usually the impact bar. The damage produced in the measurement of the force-deflection characteristics must be significantly greater than the damage to the bumper systems that were involved in the crash being investigated. The lowest failure force represents an upper limit to the peak impact force in the subject incident. The second step is to perform simulations with the numerical model that determine what closing speed is required to create an impact force that is equal to or greater than the lowest failure force. A system IF-D function can be created from the measured force-deflection data. The simulations are performed using the masses of the vehicles involved in the

actual crash. The simulations also provide the ΔV s experienced by the vehicles. The crash severity estimates obtained with this technique will provide an upper limit to the severity of the crash being investigated.

The analysis presented is for a fictional crash where Vehicle 2 is stationary and was rear-ended by Vehicle 1. Both vehicles have the same mass ($M_1=M_2=3500$ lb/g). The structural characteristics of Vehicle 2's rear bumper are represented by the force-deformation curve for the Edge bumper shown in [Fig. B3](#) and the structural characteristics of Vehicle 1's front bumper are represented by the force-deformation curve for a 2007 Kia Sportage's front bumper (see [Fig. B4](#)). The impact bar for the Sportage's front bumper failed at a force of approximately 5000 lbs in the quasi-static compression tests. The force-deformation curve for both bumpers has been approximated with the straight lines shown on the graphs in [Figures B3](#) and [B4](#) and the system IF-D function ([Eq. 11](#)) is a straight line with a slope of 18,462 lb/ft. This line is shown as a solid line in [Fig. B4](#).

If in the actual crash the plastic energy absorber of Vehicle 2 was damaged but neither impact bar was deformed, then a peak closing speed and a peak acceleration can be estimated by running the simulation model to find the impact speed for Vehicle 1 that results in a peak impact force greater than 5000 lb. In this case, the lack of damage to Vehicle 1's impact bar is being used to set an upper limit to the peak impact force. In order to maximize the ΔV for the impact the value of ϵ can be set high, although this will have no effect on the peak acceleration or the peak impact force (see [Fig. 9](#)). [Table 3](#) shows the results of this iteration procedure with $\epsilon = 0.8$. For this example the simulations indicate that if Vehicle 1 hit the rear of Vehicle 2 at a speed of 5 ft/sec the peak impact force would be 5009 lb and the impact bar in Vehicle 1 may have significant damage since this is just above the 5000 lb failure limit for this bumper's impact bar. An impact speed of 6 ft/sec would provide a more conservative estimate of the maximum impact speed and a better guarantee (taking into account bumper-to-bumper differences) that Vehicle 1's impact bar would fail. Since Vehicle 1's impact bar was not damaged in the subject incident, an impact speed of 6ft/sec provides a conservative upper limit to the impact speed of Vehicle 1 in the subject crash.

TABLE 3. Calculated peak acceleration and forces for different impact speeds of Vehicle 1.

Impact Speed (ft/sec)	Peak Impact Force (lb)	ΔV_2 (ft/sec)
4	4007	3.6
5	5009	4.5
6	6011	5.4

DISCUSSION AND CONCLUSIONS

The low-speed simulation model has been used to perform a number of parametric studies in order to understand how different variables affect the crash pulse in a low-speed crash. These parametric studies would be very difficult to replicate with actual crash testing as it would be virtually impossible to hold all of the parameters constant in a series of real crashes while only one variable was changed. The low-speed simulation model allows this type of analysis to be performed in a theoretical setting.

It is important to point out that the findings in these parametric studies are not the result of the model but are a direct result of Newton's Laws being applied in the simulated crashes. The model presented here is not necessary to reach the conclusions that are demonstrated in these parametric studies, these same conclusions could have been reached without the analytical model. The model is simply applying Newton's Laws to crash scenarios where one variable is changed in a series of simulated crashes. The model provides a tool to quantify and visualize how changing a single parameter affects the vehicle dynamics in a crash.

The first parametric study looked at how ϵ affected the crash pulse. As ϵ was increased from 0 to 1.0 the duration of the crash pulse doubled. Restitution affects the crash by allowing the deformed structures to continue to apply forces after the common velocity is reached. When ϵ equals zero there was no rebound of the deformed structures and the crash was over once the vehicles reached a common velocity. When ϵ was greater than zero the crash continued after the vehicles reached a common velocity, albeit with a continuously decreasing impact force. Thus restitution does not change the peak impact force or the peak acceleration, but it does increase the separation velocity and the ΔV experienced by each vehicle in the crash. This same conclusion was reached in the discussions of the IF-D curves shown in [Figures A2](#) and [A3](#), but as described in the preceding paragraph, the model provides a method of quantifying and demonstrating the effect of changes in ϵ on the vehicle accelerations in a crash.

The second parametric study looked at how bumper stiffness affected the crash pulse. In this parametric analysis the ϵ for the crash was kept constant by adjusting the rebound phase of the IF-D function ([Fig. 8](#)) and the pre-impact velocities were kept constant, therefore the ΔV s of Vehicle 1 and Vehicle 2 were the same in each simulation of this parametric study. Increasing the stiffness of the bumpers increased the peak accelerations and decreased the duration of the crash pulse as shown in [Fig. 10](#).

The third parametric study kept all model variables constant except for the closing speed. This analysis produced the interesting result that the pulse duration was a constant

regardless of the closing speed, and the accelerations decreased as the closing speed decreased (Fig. 11). This parametric study and the stiffness parametric study (Fig. 10) indicate that the stiffness of the bumper system determines the duration of the crash pulse for a given ϵ .

The analytical model was used to simulate three low-speed crash tests in which the dynamic IF-D curve was created from data measured during the crash tests. In order to use these data a modification was required because, as shown in Fig. 4, the force and accelerometer data approximated Newton's Second Law throughout the crash, but did not follow it exactly. When a numerical simulation of a crash test was performed with the dynamic IF-D curve an error was generated because the vehicles in the simulation had not reached a common velocity when maximum crush was reached and the rebound phase of the crash should be starting. The modification made to the measured IF-D data was to simply multiply the measured force by a constant that allowed the bullet and target vehicle to reach a common velocity in the simulation when the deformation reached the maximum deformation on the dynamic IF-D curve. This modification allowed the numerical simulations of the three crashes to be completed and the calculated accelerations and velocities were similar to the measured accelerations (Fig. 6) and velocities (Fig. 7). The accurate simulation of the three crash tests indicates that the analytical model can recreate a crash given the appropriate IF-D function.

When the simulation model is being used to recreate the dynamics of a crash or put limits on a crash that has occurred the accuracy of the calculated crash pulse depends on the IF-D function that is input into the model and how accurately this IF-D function represents the dynamic performance of the bumper systems involved in the actual crash event. The measured quasi-static force-deflection curves shown in Figures B3, B4 and B5 as solid lines were obtained with a constant deformation rate and the bumpers were taken to failure. The loading of the bumpers was done with a rigid steel beam (Fig. B2). There was also a bumper system compression test performed by replacing the steel beam with the rear bumper of a 2007 Kia Sportage and compressing a 2007 Ford Edge front bumper up to a peak force of approximately 9500 lb (dashed line in Fig. B5). Another system curve was made by adding the deformation in the quasi-static curves for the Edge's front bumper (Fig. B3) and the Sportage's rear bumper together to create a system curve for these two bumpers (dotted line in Fig. B5). Figure 12 compares these two quasi-static system curves in Fig. B5 with the measured IF-D curve in Test 3. The compression phase of the system curve obtained with the two bumpers approximates the measured IF-D curve better than the system curve made from the two separate quasi-static tests using the steel beam. This one comparison indicates that the geometry of the object applying a force to a bumper in a compression test may be important in determining the system IF-D curve

and the quasi-static data that best represents the compression phase of the dynamic IF-D curve may be obtained by measuring the quasi-static force-deformation characteristics of the both bumpers together and not individually. This is an area for future work.

Another area for future work is to determine if it is possible to develop a method to accurately quantify the rebound phase of the IF-D function based on quasi-static measurements. As shown in Fig. 12 the quasi-static system IF-D curve (dashed line) accurately portrays the compression phase of the measured IF-D curve but does not accurately portray the rebound phase. It is important to have an accurate description for the rebound phase of the IF-D function because the rebound curve determines what ϵ will be for the crash. The development of a method to define the rebound curve will require comparisons between IF-D curves obtained quasi-statically and dynamically, i.e. through crash tests for different bumper systems.

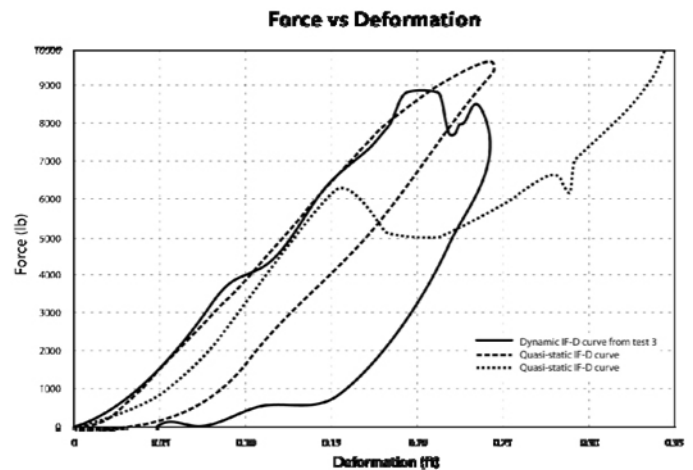


Figure 12. The dynamic IF-D curve measured in Test 3 is shown as a solid line. The IF-D curve obtained from the quasi-static compression tests with the beam is shown as the dotted line and the IF-D curve obtained by compressing the two bumpers into each other is shown as a dashed line.

REFERENCES

1. Thomson, R.W. and Romilly, D.P. "Simulation of Bumpers During Low Speed Impacts", Proceeding of the Canadian Multidisciplinary Road Safety Conference III. Saskatoon, Saskatchewan, Canada, 1993.
2. Bailey, M.N., Wong, B.C., and Lawrence, J.M., "Data and Methods for Estimating the Severity of Minor Impacts," SAE Technical Paper 950352, 1995.
3. Ojalvo, I.U. and Cohen, E.C., "An Efficient Model for Low Speed Impacts of Vehicles," SAE Technical Paper 970779, 1997.

4. Ojalvo, I.U., Weber, B.E., Evensen, D.A., Szabo, T.J. et al., "Low Speed Car Impacts with Different Bumper Systems: Correlation of Analytical Model with Tests," SAE Technical Paper [980365](#), 1998.
5. Cipriani, A.L., Bayan, F.P., Woodhouse, M.L., Cornetto, A.D. et al., "Low Speed Collinear Impact Severity: A Comparison between Full Scale Testing and Analytical Prediction Tools with Restitution Analysis," SAE Technical Paper [2002-01-0540](#), 2002.
6. Happer, A.J., Hughes, M.C., Peck, M.D., and Boehme, S.M., "Practical Analysis Methodology for Low Speed Vehicle Collisions Involving Vehicles with Modern Bumper Systems," SAE Technical Paper [2003-01-0492](#), 2003.
7. Brach, R.M., "Model of Low-Speed, Front-to-Rear Vehicle Impacts," SAE Technical Paper [2003-01-0491](#), 2003.
8. Collins, J.C. "Accident Reconstruction", Charles C. Thomas, Springfield, Illinois, USA, 1979.
9. 2008 Mitchell Collision Estimating & Reference Guide, Mitchell International, 9889 Willow Creek Road, San Diego, CA.

CONTACT INFORMATION

William R. "Mike" Scott
Biodynamic Research Corporation
5711 University Heights Blvd., Suite 100
San Antonio, Texas 78249
Phone: (210) 691-0281
Fax: (210) 691-8823
mscott@brconline.com

A copy of the Matlab7 code used in the parametric studies will be e-mailed upon request.

ACKNOWLEDGMENTS

The authors acknowledge the work of Mr. Enrique Bonugli and Mr. Herb Guzman for performing the quasi-static measurements on the bumper systems presented in this paper and for performing the crash tests. The authors also thank Mr. Jimmy Cosgrove and Mr. Bob Carlin for creating the illustrations.

The authors would also like to thank the reviewers for their comments and suggestions as well as for the time that they spend reviewing this manuscript.

APPENDIX A

ENERGY DEFINITION OF THE COEFFICIENT OF RESTITUTION

A two vehicle system composed of Vehicle 1 and Vehicle 2 has a common center of mass that is located between the two vehicles and moves with the vehicles. If the masses of Vehicle 1 and Vehicle 2 are M_1 and M_2 , then the mass of the common center of mass is M_1+M_2 . If the velocity of Vehicle 1 and Vehicle 2 are V_1 and V_2 then the velocity of the common center of mass (V_{cm}) is,

$$V_{cm} = (M_1 V_1 + M_2 V_2) / (M_1 + M_2) \quad (1A)$$

In a crash V_{cm} does not change because of conservation of momentum. The common center of mass also has a kinetic energy (KE) associated with it,

$$E_{cm} = \frac{1}{2} (M_1 + M_2) V_{cm}^2 = \frac{1}{2} (M_1 V_1 + M_2 V_2)^2 / (M_1 + M_2) \quad (2A)$$

Since V_{cm} does not change in a crash, E_{cm} also does not change. The system of two vehicles also has a pre-crash KE which is the sum of the KE of each vehicle,

$$E_{sys} = \frac{1}{2} M_1 V_1^2 + \frac{1}{2} M_2 V_2^2 \quad (3A)$$

The KE of the system is greater than E_{cm} and the difference is E_{afc} ,

$$E_{afc} = E_{sys} - E_{cm} = \frac{1}{2} M_1 M_2 (V_1 - V_2)^2 / (M_1 + M_2) \quad (4A)$$

where E_{afc} is the amount of energy available for crush and for heat generation in the two car system pre-crash (8). For this analysis it is assumed that the heat generated in a crash is negligible and it is neglected. Usually only some of E_{afc} is used up in a crash and after the vehicles separate there is still some energy, E_{afc}^* , in the system that can be used for crush. If the post-crash velocities of Vehicle 1 and Vehicle 2 are V_1^* and V_2^* , then

$$E_{afc}^* = \frac{1}{2} M_1 M_2 (V_1^* - V_2^*)^2 / (M_1 + M_2) \quad (5A)$$

The energy definition of the coefficient of restitution is ϵ^2 equals the fraction of E_{afc} that was not used in the crash to create heat or crush metal (8), and

$$\epsilon^2 = E_{afc}^* / E_{afc} \quad (6A)$$

When Eqs. 4A and 5A are substituted into Eq. 6A for E_{afc}^* and E_{afc} , the result is Eq. 9. Eq. 9 describes the effect of restitution on post-crash velocities. Eq. 6A describes how the energy balance in the system is influenced by the restitution in the crash.

Figure A1 graphically shows the kinetic energy allocation in a collinear two vehicle system before and after a crash. In this system Vehicle 2 is initially stationary ($V_2=0$) and Vehicle 1 impacts the rear of Vehicle 2 with velocity V_1 . The masses of Vehicle 1 and 2 are taken to be equal. Prior to the crash, $E_{sys} = \frac{1}{2} M_1 V_1^2$ (Eq. 3A). One half of the system KE is in the center of mass motion, $E_{cm} = \frac{1}{4} M_1 V_1^2$ (Eq. 2A), and the other half of

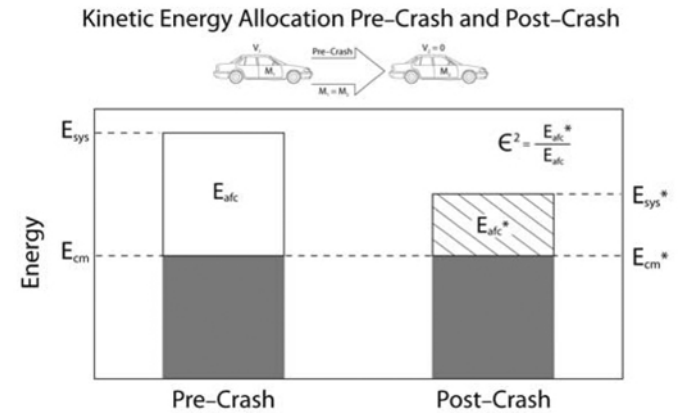


Figure A1. The kinetic energy distribution in a two vehicle system before the crash and after the crash.

the system KE is available for crush, $E_{afc} = \frac{1}{4} M_1 V_1^2$ (Eq. 4A). Post-crash E_{cm} has not changed, but the energy available for crush in a subsequent impact, E_{afc}^* , has decreased. The ratio between the amount of energy available for crush post-crash (E_{afc}^*) to the amount available pre-crash (E_{afc}) is equal to ϵ^2 as described in Eq. 6A (8). The lost KE has gone into the work of crushing the vehicle bumper systems.

The energy definition for ϵ indicates that the force-deformation characteristics of the vehicles structures that make contact in the crash determine ϵ for that crash. The Impact Force-Deformation curves in Figs. A2 and A3 illustrate this concept in two crashes. Deformation is made up of crush, which is permanent and elastic deformation. The deformation in Figs. A2 and A3 represents the sum of the deformation of both vehicles at a given impact force. Fig. A2 represents a crash where most of the deformation is permanent crush and Fig. A3 represents a crash with the same

initial conditions but the majority of the deformation is elastic. Once the vehicles make contact the structures will deform and an impact force will be created that acts on both vehicles. If the impact force and deformation at a given time in the crash are plotted on the Impact Force vs. Deformation coordinate system the points will form a curve that moves over the plane of the coordinate system with time. As long as the deformation continues to increase the Impact Force-Deformation curve will move to the right on

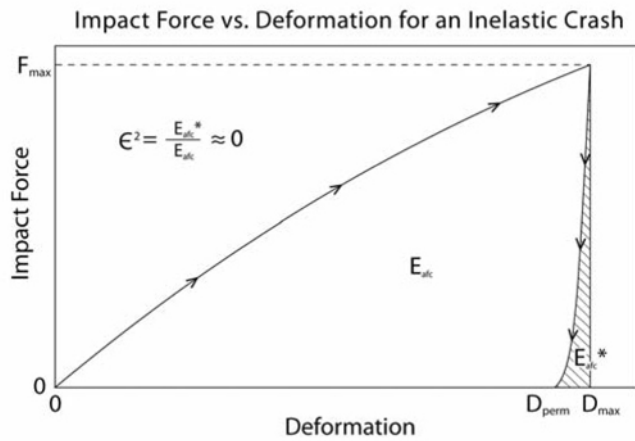


Figure A2. The impact force-deformation curve for a crash where there is little rebound of the bumper structures during the crash. E_{afc} is the area under the upper curve from 0 to D_{max} . E_{afc}^* is the shaded area.

the diagram. The Impact Force-Deformation curve will continue to the right until the vehicles reach a common velocity and the deformation is at a maximum (D_{max}). Since both vehicles have the same velocity at this point in the crash, they are in a situation, at least temporarily, where $\epsilon = 0$, and all of E_{afc} has been used up to create the deformation up to D_{max} . Therefore, the area under the Impact Force-Deformation curve up to D_{max} must equal E_{afc} . In high speed crashes or crashes where the vehicles have inelastic structures this is the end of the crash, ϵ is approximately zero and the impacting vehicles depart the crash with similar velocities. This situation is depicted in [Fig. A2](#) where the Impact Force-Deformation curve after D_{max} has a steep slope and the permanent crush, D_{perm} , is just slightly less than D_{max} . In this situation almost all of the energy available for crush, E_{afc} , has been used to crush the two vehicles and $\epsilon^2 \approx 0$.

The situation is very different when the deformed structures are more elastic because the crash is not over once the vehicles reach a common velocity. [Fig. A3](#) illustrates the same crash as shown in [Fig. A2](#) except that the deformed structures are more elastic. The path up to D_{max} is the same as in [Figure A2](#), but after D_{max} is reached the deformed structures rebound a significant amount and the permanent crush is a fraction of the maximum deformation. The work

done by the rebounding structures is E_{afc}^* and this energy is returned to the system. This returned energy increases the separation velocity ($V_1^* - V_2^*$), the system kinetic energy and the ΔV experienced by each vehicle in the crash.

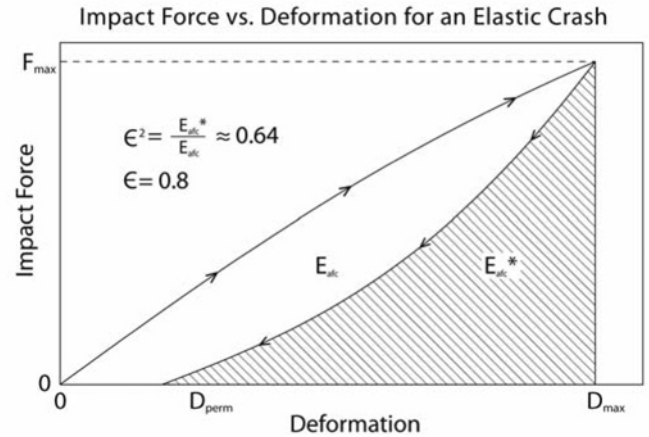


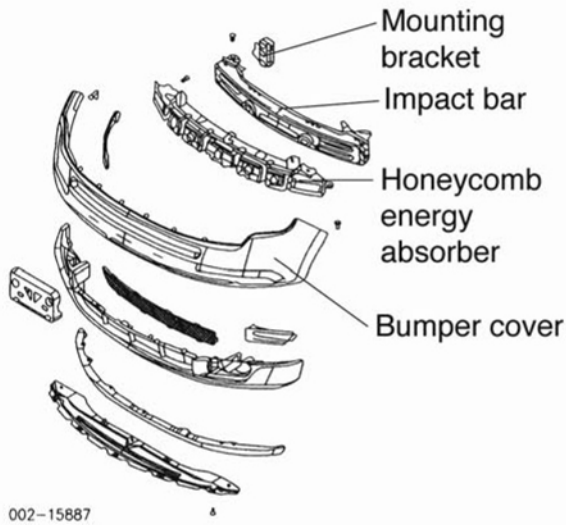
Figure A3. The impact force-deformation curve for a crash where there is significant rebound of the bumper structures during the crash. E_{afc} is the area under the upper curve from 0 to D_{max} . E_{afc}^* is the shaded area.

APPENDIX B

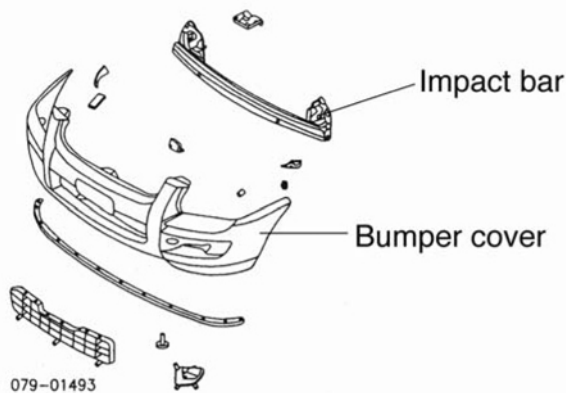
DESCRIPTION OF THE BUMPERS USED IN THE CRASH TESTS AND SIMULATIONS

Static-force deflection measurements were made on three bumpers for this study. The three bumpers are the front bumper of the 2007 Ford Edge and the front and rear bumper of the 2007 Kia Sportage. Schematics for the three bumpers are shown in [Fig. B1](#) (9).

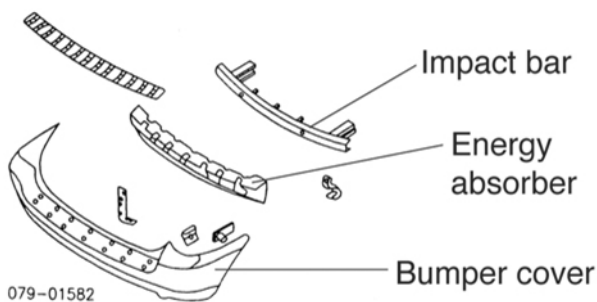
The Edge front bumper is constructed of a curved metal impact bar with a honeycomb plastic energy absorber placed between the impact bar and the plastic cover as shown in [Fig. B1](#). The Sportage's front bumper has a metal impact bar with no energy absorbing element between the impact bar and the cover, as shown in [Figure B2](#). The Sportage's rear bumper has a curved composite impact bar with a cover. There is an energy absorbing foam material on the top of the impact bar, but this foam material only covered approximately the top 1.5 inches of the rear surface of the impact bar. This foam appears to be designed as a vertical support for the bumper cover so that people can step on or place objects on the top of the rear bumper.



2007 Ford Edge Front Bumper



2007 Kia Sportage Front Bumper



2007 Kia Sportage Rear Bumper

Figure B1. Schematics of the bumpers used in this study.

The static force-deformation characteristics of the bumpers were measured by mounting the bumper onto a rigid base using the same brackets that are used to attach the bumper to the vehicle body. The center of the test bumper was compressed by a beam that had a curved surface similar to a bumper's shape and a width of 2.5 inches. The beam was attached to a hydraulic piston. The rate of compression was

approximately 0.075 ft/sec. The compression force was measured with a load cell attached to the top of the beam (Model 1210A-25k, Interface Corp.) and the displacement was measured with a displacement transducer (LVDT type, LH series, MTS, Inc.). Figure B2 shows the shape of the steel beam used to compress the bumpers along with the Edge's impact bar and honeycomb energy absorber without the bumper cover. The load cell is mounted directly over this beam.

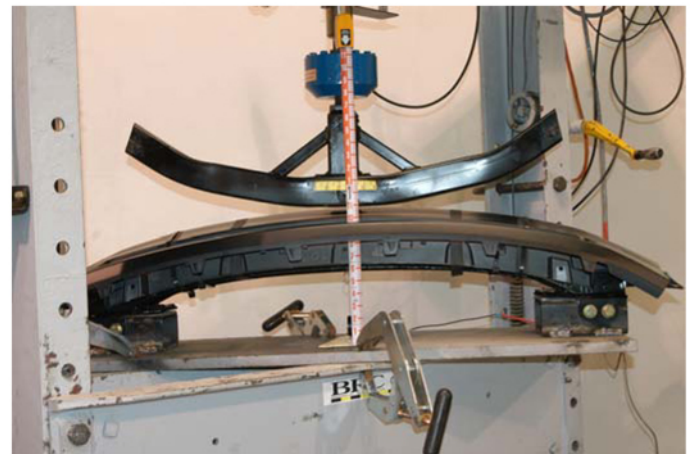


Figure B2. Photograph of the test setup used to measure the force-deformation characteristics of the bumpers.

Figure B3 shows the quasi-static force-deformation curve measured on a new 2007 Ford Edge front bumper. The bumper was compressed until the impact bar failed. The first 0.021 ft of deformation in the compression phase of the curve represents the crush of the plastic energy absorber. The slope of the force-deformation curve increased after the plastic energy absorber was crushed. The force increased until approximately 22,000 lbs when the impact bar failed and further compression resulted in a decrease in the force. The dashed straight line (slope = 48,000 lb/ft) in Fig. B3 approximates the compression phase of the force-deformation curve of the Edge's bumper. The solid straight line (slope = 24,000 lb/ft) in Fig. B3 represents a system IF-D function of a bumper system that is composed of two bumpers that have a linear stiffness of 48,000 lb/ft (Eq. 11).

Figure B4 shows the quasi-static force-deformation curve measured on a new 2007 Kia Sportage front bumper. The impact bar completely failed at a force of approximately 5000 lb. The compression part of the force-deformation curve in Fig. B4 has been approximated with a line that has a slope of 30,000 lb/ft. When this linear force-deformation curve is combined with the linear force-deformation curve for the Edge (48,000 lb/ft) the system IF-D function (Eq. 11) is a straight line with a slope of 18,462 lb/ft. This IF-D function is shown as a solid straight line in Fig. B4.

Figure B5 shows the quasi-static force-deformation curve measured with a new 2007 Kia Sportage rear bumper as a solid line. This test was performed without the foam energy absorber that covered the top rear surface of the impact bar because the discontinuity in the surface could have produced a bending moment that may have damaged the load cell. The force increased until it reached approximately 17,500 lbs when there was a load noise and the composite impact bar cracked. The dotted line in Fig. B5 is a system compression IF-D function made by adding the deformation in the compression phase of the force-deformation curve for the Edge's front bumper and the Kia Sportage's rear bumper for forces up to 10,000 lb. There is no data available from our measurements to construct a rebound phase for this system IF-D function so only the compression phase is shown. Another system IF-D curve was produced by replacing the compression beam shown in Fig. B2 with a new Kia Sportage rear bumper and using this bumper to compress a new Ford Edge front bumper. The two bumpers were compressed up to approximately 9,600 lbs and then the force was released. The system force-deformation curve measured in this test is shown in Fig B5 as a dashed line. The quasi-static force-deformation curve obtained with the two bumpers is stiffer than the curve obtained by combing the two quasi-static tests. The difference appears to reflect the geometrical difference between the steel bar and the Sportage's rear bumper. The steel bar is narrower and has a smaller contact area than the Sportage's rear bumper. The reduced contact area may allow the beam to crush the honeycomb plastic at a lower force than the Sportage's bumper.

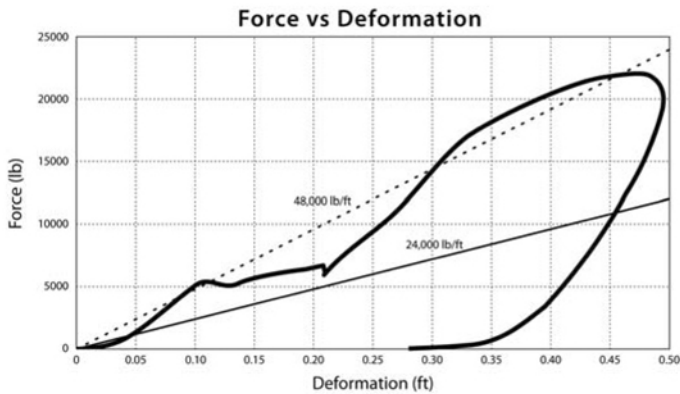


Figure B3. The quasi-static Force-Deformation curve for the Edge's front bumper. The dashed line is a linear approximation of the upper part of the curve and the solid line represents the compression phase of a system IF-D function for a simulation where both bumpers have the stiffness defined by the dashed line.

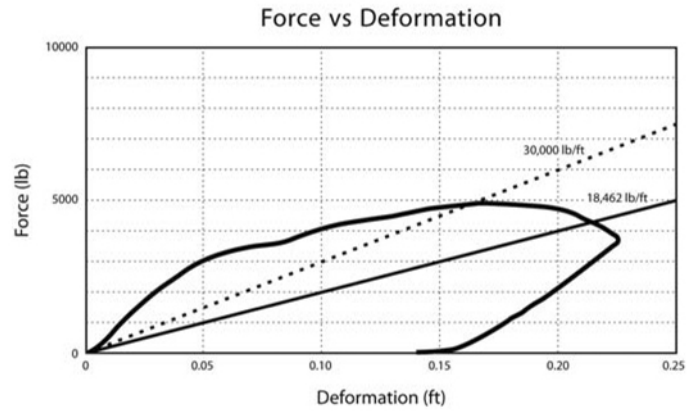


Figure B4. The quasi-static Force-Deformation curve for the Sportage's front bumper. The dotted line is a linear approximation of the upper part of the curve and the solid line represents the compression phase of a system IF-D function that has a stiffness of 18,462 lb/ft.

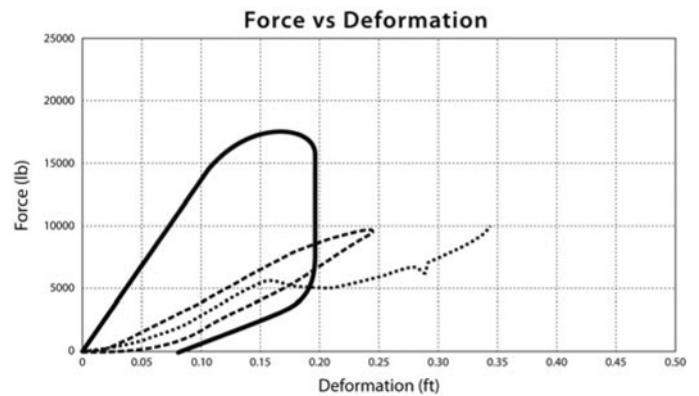


Figure B5. The quasi-static Force-Deformation curve for the Sportage's rear bumper is shown as a solid line. The dotted line is the quasi-static compression Force-Deformation curve made by combining the curve for the Edge's front bumper and the Sportage's rear bumper. The dashed line is the measured quasi-static Force-Deformation curve obtained by compressing the Sportage's rear bumper into the Edge's front bumper.

The Engineering Meetings Board has approved this paper for publication. It has successfully completed SAE's peer review process under the supervision of the session organizer. This process requires a minimum of three (3) reviews by industry experts.

All rights reserved. No part of this publication may be reproduced, stored in a retrieval system, or transmitted, in any form or by any means, electronic, mechanical, photocopying, recording, or otherwise, without the prior written permission of SAE.

ISSN 0148-7191

doi:[10.4271/2010-01-0051](https://doi.org/10.4271/2010-01-0051)

Positions and opinions advanced in this paper are those of the author(s) and not necessarily those of SAE. The author is solely responsible for the content of the paper.

SAE Customer Service:

Tel: 877-606-7323 (inside USA and Canada)

Tel: 724-776-4970 (outside USA)

Fax: 724-776-0790

Email: CustomerService@sae.org

SAE Web Address: <http://www.sae.org>

Printed in USA

SAE *International*[™]